

Hydroclimatic analysis of an ice-scar tree-ring chronology of a high-boreal lake in Northern Québec, Canada

Mickaël Lemay and Yves Bégin

ABSTRACT

Ice-scars were investigated to reconstruct the ice-flood history of Corvette Lake in Northern Québec in an attempt to determine the hydrological threshold of shore ice and identify the accompanying climatic conditions. The ice-scar record started around 1850 and showed a rapid increase in frequency at the start of the 1930s, while trees damaged by the ice were already mature and established over several decades. The study supports the hypothesis that this shift could correspond to an increase in flood discharge. Hydrological analysis of every event that occurred since 1961, the year during which instrumental recording began, indicated that scar frequency and scar maximum height were strongly correlated with average recession discharge, average flood discharge, peak discharge and flood onset. Ice-scars provided a discontinuous record of discrete events triggered by hydrologic extremes that were used to document the instrumental record using logistic regression. Results from multiple regressions suggested that ice-scars correspond to years with highs in total precipitation from January to March and from May to June, in the sum of degree-days of frost in April, and in the sum of degree-days of heat from October to April. Although imperfect for reconstructing past events, this study exemplifies the potential use of ice-scars for extending the historical record of ice-floods with hydroclimatic significance.

Key words | break-up, hydrograph, ice-scar chronology, lake ice, spring flood, tree-rings

Mickaël Lemay (corresponding author)
Centre d'Études Nordiques and Department of
Geography,
Laval University,
Québec G1V 0A6,
Canada
Tel.: +1 418 656 3340
Fax: +1 418 656 2978
E-mail: mickaël.lemay.1@ulaval.ca

Yves Bégin
Centre d'Études Nordiques and Centre Eau,
Terre et Environnement,
Institut National de la Recherche Scientifique,
Québec G1K 9A9,
Canada

INTRODUCTION

Dendrohydrology, the study of hydrological processes using tree rings (Schweingruber 1996), yields indications of past hydrological events that affected the growth of trees. Years of shore erosion events that caused tree leaning, scouring, breaking or bending of tree stems are generally well recorded in annual ring sequences and can be used to reconstruct past disturbances on river banks and lake shores (Lepage & Bégin 1996; Bégin 2000c). Among dendrohydrologic markers, ice-scars have proven to be proxy indicators of past spring floods. Given that approximately 40% of precipitation falls as snow in the boreal and subarctic zones, spring events account for a large part of the total run-off (Karl *et al.* 1993). Bégin (2000c) improved the methodology of using ice-scars on trees to date past extreme

lake levels. On large water bodies of the subarctic zone, lake ice covers are still complete when snowmelt occurs. Open water at the edge of the ice allows the wind to slightly displace lake ice, causing it to damage shoreline trees by scarring and bark removal. Such damage, when replicated among several trees and among several sites, and when not involving onshore ice-ridge formation, is significant as an indicator of lake levels (Dionne 1979).

The abrasion of the bark by the ice damages the “cambium”, which is composed of the living cells of wood that divide and create the annual tree rings. At the position of damage the disrupted cambium ceases cell division. The addition of wood at its intact edges creates a callous margin that contains a number of annual rings equivalent to the age

doi: 10.2166/nh.2008.003

of the scouring event. The resulting scars constitute a record of ice events (Alestalo 1971; Alestalo & Häikiö 1975; Shroder 1980; Smith & Reynolds 1983; Bégin & Payette 1988; Schweingruber 1996). Several studies have used such ice-scars to date past spring high water events and interpret their significance in terms of hydrological history. Ice-scars as proxy indicators of spring flood magnitude have been successfully used in numerous studies conducted in north-eastern Canada, particularly in the Boniface River region at the tree line (Payette & Delwaide 1991), in Clearwater Lake in the forest-tundra (Bégin & Payette 1988), in Bienville Lake in the high boreal zone (Lepage & Bégin 1996; Bégin 2001) and in Duparquet Lake at the southern limit of the boreal forest (Tardif & Bergeron 1997). A general rising trend of extreme lake levels was consistently observed during the 20th century, which was interpreted by authors as the result of an increase in snowfall. Although these studies present many attempts to decipher a climatic signal in ice-scar chronologies, the hydroclimatic significance of ice-scouring chronologies remains relatively ambiguous and needs to be clarified in order to integrate this proxy indicator as a discrete parameter in hydroclimatic modeling.

In this study, ice-scars were investigated to reconstruct the ice-flood history of Corvette Lake, located in the James Bay region of northern Québec. We hypothesized that drifting ice activity reflects some specific features of the regional spring flood hydrograph, which are influenced by winter precipitation and by the climatic conditions prevailing at the time of break-up. Our study had three specific objectives: (1) to compare the ice-flood history of Corvette Lake with other chronologies from north-eastern Canada; (2) to determine the spring flood hydrograph variables that are associated with ice-push events and (3) to identify the hydroclimatic conditions leading to ice activity.

METHODS

Study area

Corvette Lake has only one outlet (Corvette River) located at its north-west extremity that drains towards Pontois River, which supplies the La Grande 3 (LG3) reservoir (Figure 1). Like most large northern lakes, the level of

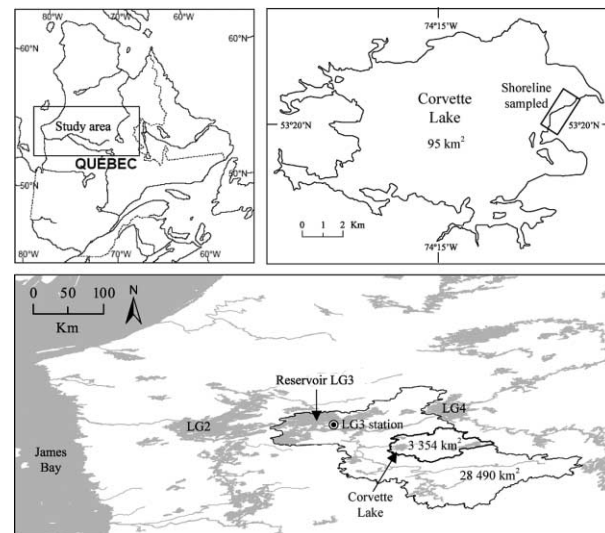


Figure 1 | Study area with the catchments of Corvette Lake and the La Grande 3 (LG3) reservoir. The black lines mark the boundaries of LG3 and Corvette Lake (bold line) watersheds; the areas (km²) covered by the watersheds and the Corvette Lake are indicated on the map.

Corvette Lake reaches its maximum at the spring flood, decreasing progressively during summer until September and then dropping to its minimum during winter due to snow retention.

According to the data recorded (from 1960 to 2006 on a daily basis) at the LG3 meteorological station (about 70 km north-west of Corvette Lake), the mean annual temperature is -3.8°C and the maximum monthly mean (13.7°C) is reached in July, while the minimum monthly average (-23.6°C) occurs in January. The total annual precipitation is 798 mm, with about 35% (282 mm) falling as snow. Corvette Lake is located approximately at the isotherm of 700 growth degree-days ($>5^{\circ}\text{C}$). The vegetation surrounding Corvette Lake is open boreal forest dominated by black spruce (*Picea mariana* Mill., BSP) in wet areas and Jack pine (*Pinus banksiana* Lamb.) in well-drained areas (Lavoie & Sirois 1998).

Field sampling and construction of the ice-scar chronology

A 2 km long shore stretch was first surveyed for ice-scars on riparian black spruce trees (dead or alive). Because geomorphologic and ecological impacts of ice-pushes vary greatly along lake shorelines according to site exposure (Bégin

2000b), the section was segmented into homogeneous segments on the basis of geomorphologic and ecological features to define a typology and characterize the ice activity regime of every type of shore. All sites favorable to ice-ridge formation were systematically eliminated since they are not reliable indicators of the spring flood lake hydrology. Such highly exposed shores are usually capes and are characterized by steep slopes, unstable boulder ridges, discontinuous tree stands and tilted trees with long ice-scars, which are geomorphologic evidence of ice-ridge formation. Following the methodology of Bégin (2000c), only shore segments of intermediate exposure characterized by continuous riparian tree stands were considered to build the ice-scar chronology. These corresponded to 15 shore sections that covered 75% of the total shoreline investigated. All trees with visible scars were sampled and some trees not presenting any visible scars were also cut to assess if they bore any hidden scars.

The second step consisted of compiling the dated scars for every linear shore segment of 10 m. Within these segments, dates of disturbance were considered, regardless of the number of trees affected, to avoid the overweighting of events due to the stand density. Every tree sampled was precisely mapped with a theodolite (maps were produced with MapInfo) to perform the second step of event listing. Finally, to be included in the chronology, an ice-push event had to be represented by at least two scars within the entire shoreline investigated, in order to eliminate scars that could potentially result from disturbance agents other than ice activity (Bégin 2000c).

Cross sections were taken in the middle of the scars and as close as possible to the collar/ground level. An average of two cross sections was taken for every tree sampled. Samples were dried and finely sanded prior to examination under a dissecting microscope. Light rings, narrow rings, incomplete rings and frost rings were listed on every sample. These diagnostic rings allowed preparation of a skeleton plot according to the method described by Schweingruber (1988), in order to date and cross-date the samples. Tree establishment was dated from the collar sections to ensure that riparian tree line stands were present at the beginning of the period covered by the chronology.

At the end of the selection process, 353 of the 501 scars dated on 231 of the 287 trees sampled were used to build the ice-scar chronology. The chronology is presented in a

histogram showing the relative ice-scar frequency bars weighted by the relative number of trees available (providing a record at year t) according to Shroder's formula (1978). This is done to extract the damping trend with time of the decreased survival of older trees on the number of ice-scars. Hereafter, the relative scar frequency is referred to as the index of weighted scar frequency.

Shroder's formula does not take into account the effects of ice disturbance on the bearing tree population's demography. In other words, any severe ice activity may destroy the past record by eliminating the trees or may limit tree regeneration and the potential for future recording. When using the formula, tree population demography can be accounted for by selecting sites with intermediate exposure, where ice exposure features allow for tree survival and regeneration. A Kolmogorov–Smirnov test was used to evaluate the independence of the ice-scar age structure with that of the bearing tree population. To discriminate against the possibility of unrecorded events due to the high flexibility of the young black spruce stem, only trees of more than 20 years of age were considered, corresponding to a stem diameter of approximately 5 cm.

Measurement of ice-scars

The height and length of every visible ice-scar on shore trees were measured with a metric tape. Their elevation was also measured with a theodolite and the lake level of 20 June 2000 was used as a reference. Scars longer than 50 cm were systematically excluded from the height analysis since they may be associated with ice piling or ice sliding on the stem. Given that lake level can vary during the flood, the heights of flood levels were determined according to the maximum height value recorded for each ice-push event (Harrison & Reid 1967; Parker & Jozsa 1973; Payette 1980; Tardif & Bergeron 1997; Bégin 2000c). This single elevation value for each event was correlated with scar frequency in order to distinguish years of major ice-push events.

Hydrologic and climatic data analysis

Hydrologic and climatic data were available from a Hydro-Québec station located on the LG3 reservoir covering the period from 1961 to 1999 on a daily basis. The hydrologic

record is separated into two periods. From 1961 to 1980 water supplies to the LG3 reservoir were estimated from the gauged record of tributaries. However, during this period the hydrological series were modeled on a daily basis using the daily climatic record and calibrated with the regional hydrological reference series of the Harricana River located further south. From 1980 to 1999, water supply values were gauged directly on the LG3 reservoir and were adjusted so that the water inputs coming from upstream reservoirs were not included. The resulting data series are called “harmonized water supply to basin” and represent the best estimates that are used for day-to-day predictions for water management by Hydro-Québec.

Ten hydrographical variables (listed in Table 1) were considered in describing the floods according to Gregory & Walling (1973). It should be noted that the flood end corresponds to the day that discharge decreased below $635 \text{ m}^3/\text{s}$ (mean summer discharge measured on the LG3 reservoir). However, the ice cover is no longer present after June in this region. Therefore, the end of recession was defined as the last day of June where the discharge was higher than $635 \text{ m}^3/\text{s}$. The variables “flood duration” and “duration of recession” should be interpreted as the effective period when ice-push was possible.

The relationship between ice activity (weighted frequency and height of ice-scars) and the spring hydrograph variables

was tested using Spearman’s ranked correlation coefficients since the ice activity variables were non-parametric. Years without recorded ice-push events were included in the analysis. Further analyses were required to refine and quantify this relationship. Independent sample *t*-tests were used to quantify differences between years with and without ice-scars for every correlated hydrograph variable. Logistic regression was performed with the absence/presence of ice-scars as the dependent variable in order to identify a threshold value for each correlated hydrograph variable for ice activity. The threshold values were determined to maximize the predictive value of the model in discriminating between years with and without ice activity. The logistic regression allowed the calculation of the relative risk (or risk ratio, from the classification table) to compare the relative likelihood of an event (ice-push) occurring between two distinct groups (determined according to the threshold value).

Finally, the relationship between hydrologic data and climatic variables (spanning a period of 39 years) was tested using multiple regressions with the stepwise selection and the bootstrap verification method (1000 iterations) (Efron 1979). The method used was a canonical regression, which eliminated autocorrelation between climatic variables included in the same multiple regressions (Guiot *et al.* 1982). Results of the multiple regressions were expressed by the partial regression coefficients (Fritts *et al.* 1971). These analyses were performed with the CALROB program included in the 3PBase package (Guiot 1999). The climatic variables tested were minimum, maximum and mean temperatures, snowfall, rainfall and total precipitation, sum of degree-days of frost ($<0^\circ\text{C}$) and sum of degree-days of heat ($>0^\circ\text{C}$). Data from September to June were used to elaborate the climatic variables for each of the 39 years (1961–2000). Climatic analysis of spring flood periods was conducted using monthly hydrological data to avoid the circular problem related to the daily hydrological data of the period from 1961 to 1980 previously mentioned (e.g. climatic input in the daily spring hydrograph modeling). Accordingly, water inputs of May and June were considered for the multiple regressions. Precipitation variables were systematically divided into two periods (January–March and April–June) to compare the impact of spring precipitation (mostly rainfall) with the impact of winter precipitation (snowfall). Moreover, the climatic

Table 1 | Spearman’s correlations between hydrograph variables and ice activity

Hydrograph variables	Scar frequency	Maximum scar height
Mean flood discharge (m^3/s)	0.625*	0.583*
Mean recession discharge (m^3/s)	0.592*	0.569*
Peak discharge (m^3/s)	0.407 [†]	0.419*
Slope of hydrograph rise	Ns	Ns
Flood onset (d)	0.507*	0.423*
Peak timing (d)	Ns	Ns
End of flood (d) [‡]	0.530*	0.471*
Flood duration (d)	Ns	Ns
Duration of recession (d)	Ns	Ns
Time to peak (d)	Ns	Ns

Ns: Non-significant, $n = 39$.

* $p < 0.01$.

[†] $p < 0.05$.

[‡]The last day of the flood event was defined by default as the last day of June during which the discharge was higher than $635 \text{ m}^3/\text{s}$.

variables retained by the stepwise selection and periods over which they had a significant influence on water inputs were combined into “climatic-period” variables in order to simplify the models.

RESULTS

Ice-scar frequency and elevation

The ice-scar chronology of Corvette Lake spanned the period of 1850 to 2000 (Figure 2). Riparian trees recorded 56 years of ice-push events during this period. The chronology showed that ice activity increased between 1850 and 2000 and revealed that the number of ice-scar years, at first sporadic and irregular, became more frequent and recurred regularly during the 20th century. Indeed, only 12 years of ice-push events were recorded prior to 1925, while 44 occurred afterward. The frequency of years of ice-push events was 1.9 per decade prior to 1930, but increased to 5.9 after 1930. A significant Kolmogorov–Smirnov test between both cumulative curves of tree establishment and scar weighted frequency indicated that the record of ice-scars was independent of the age structure of the bearing riparian tree stands (Figure 3).

The yearly maximum ice-scar height was strongly correlated with the weighted ice-scar frequency ($r_s = 0.896$, $p < 0.01$; Figure 2). Years marked by the most abundant ice-scars were also those of maximum water levels. These two parameters enabled identification of the years 1947, 1952, 1956, 1957, 1959, 1979, 1981 and 1989 as being years during which severe ice-push events occurred.

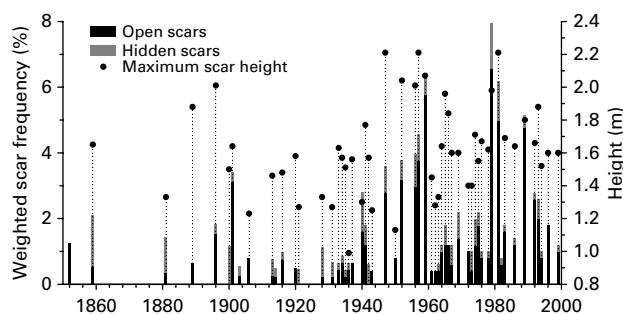


Figure 2 | Ice-scar chronology of Corvette Lake. The weighted frequency and the maximum scar height are strongly correlated ($r_s = 0.896$; $p < 0.01$).

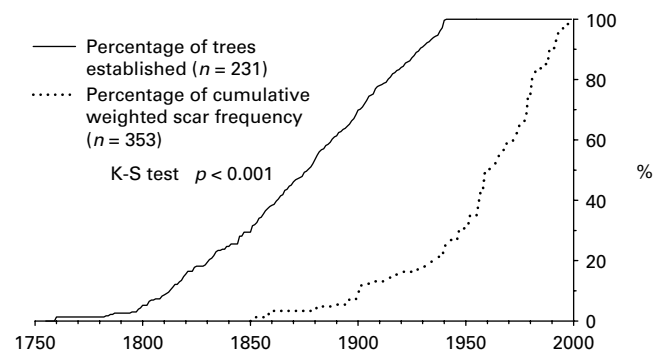


Figure 3 | Comparison of the cumulative percentage for both ice-scar weighted frequency and tree establishment (trees aged greater than 20 years).

Relationship between ice-scouring and spring flood hydrograph

Both ice-scar frequency and maximum height were positively correlated with the magnitude of floods, except for the slope of hydrograph rise (Table 1). The strongest correlation for both ice-scar frequency and maximum height was with mean flood discharge (Figure 4). There was no statistical relationship with any aspect of flood duration. However, the period of flood occurrence appeared to influence ice-push development. In almost all cases, ice-scar frequency was most strongly correlated to hydrograph variables, except for peak flood discharge, which showed a slightly stronger correlation with ice-scar maximum height.

Quantifying differences between floods that did or did not lead to ice activity

The t -tests comparing the presence ($n = 25$) and absence ($n = 14$) of ice activity revealed that the mean flood discharge and mean recession discharge were higher during years of ice activity (Table 2). Moreover, years with ice activity were characterized by a notably higher peak discharge than years without ice-scouring. Floods leading to ice-push development typically began and ended later than those without ice-push, but did not necessarily reach their maximum later. In many cases, the end of recession corresponded to the end of June and consequently the duration of the effective period of drifting ice activity did not vary significantly from year to year. However, it should

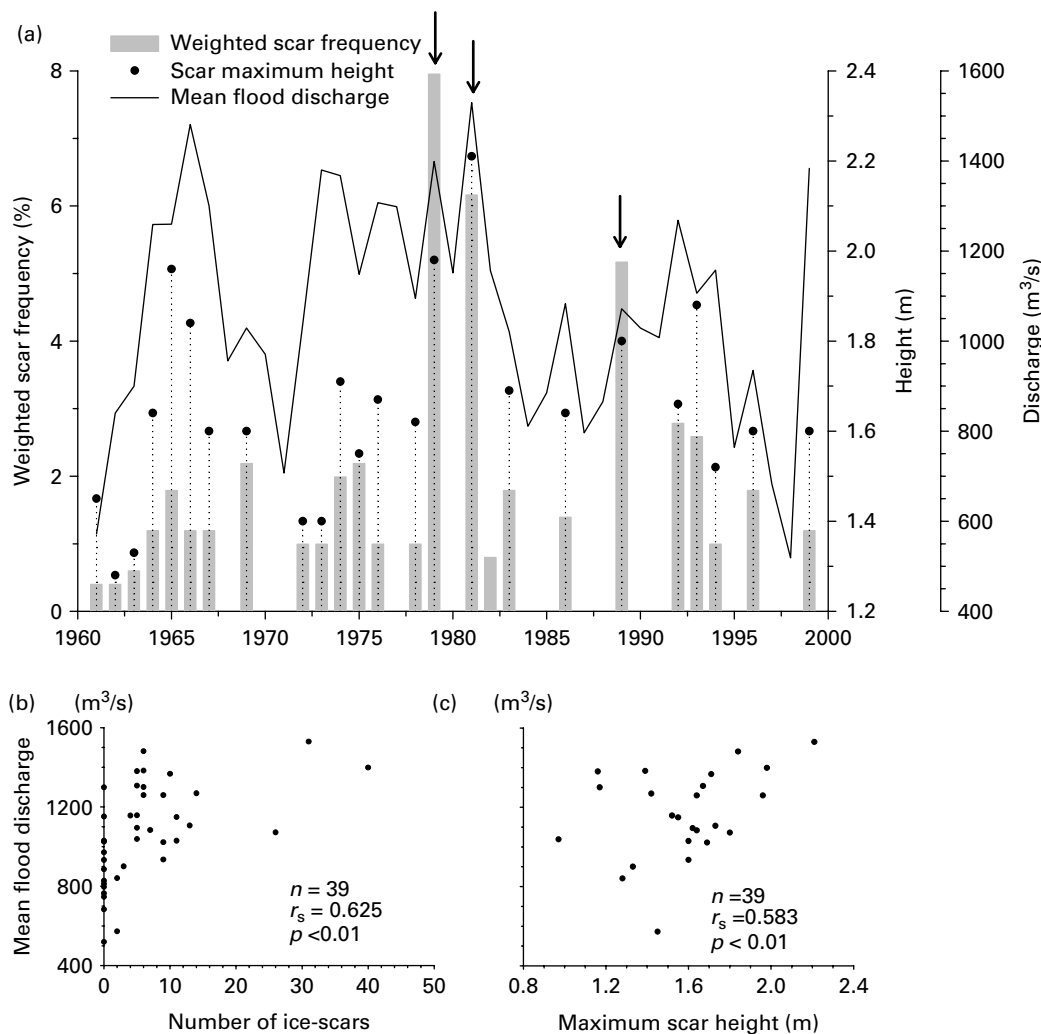


Figure 4 | Relation between the mean flood discharge (line) and the weighted ice-scar frequency and maximum scar height (a). Arrows represent years of severe ice-push events. Scatter plots represent the distribution of both ice-scar frequency (b) and scar height (c) according to the mean food discharge.

be noted that water inputs at the end of June (e.g. at the end of recession) were significantly higher ($289 \text{ m}^3/\text{s}$; $p = 0.001$) for years with ice activity (result not included in Table 1).

The mean hydrograph curves of years identified as severe ice-push events (Figure 5(a)) were generally characterized by a higher mean recession and mean flood discharge than typical ice activity years. Indeed, the

Table 2 | Individual t-tests quantifying mean differences in hydrograph variables between years with and without ice activity

Hydrograph variables	p value	Mean difference	Standard deviation
Mean flood discharge (m^3/s)	0.000	-274.6	68.9
Mean recession discharge (m^3/s)	0.005	-228.2	75.5
Peak discharge (m^3/s)	0.022	-378.2	157.6
Flood onset (d)	0.001	-10.8	3.09
Flood end (d)	0.001	-10.0	2.52

Years with ice activity, $n = 25$. Years without ice activity, $n = 14$.

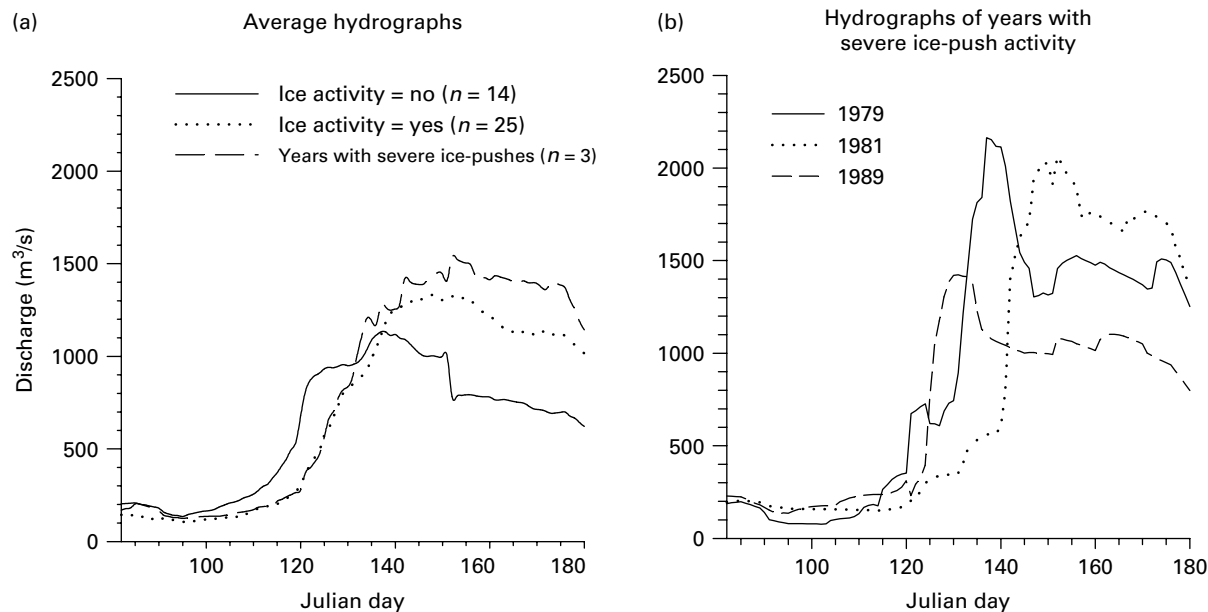


Figure 5 | Average regional hydrographs for years without ice-scars, years with minor and severe ice activity (a) and regional hydrographs for specific years marked by severe ice activity (b).

hydrographs of 1979 and 1981 showed that these flood levels were exceptionally high and that the inputs of water following the flood peak were maintained (Figure 5(b)). However, the flood of 1989 did not reach a particularly high magnitude and was not sustained.

Hydrological significance of the occurrence of ice activity

Threshold values discriminating between years with and without ice activity were determined for four hydrograph variables using logistic regression (Figure 6). Results indicated that the probability of ice-push development associated with a mean flood discharge exceeding $1030 \text{ m}^3/\text{s}$ was 62% (Figure 6(a)). Logistic regression also revealed that there was 68% less chance of ice-push if the flood began prior to Julian day 121 (Figure 6(b)). The threshold value identified for mean recession discharge was $1065 \text{ m}^3/\text{s}$, corresponding to a probability of 52% (Figure 6(c)). Finally, a flood reaching over $1255 \text{ m}^3/\text{s}$ at its peak was associated with a 56% probability of ice-scouring (Figure 6(d)).

Nineteen hydrographs exceeded the four threshold values and only one of them (year 1977) did not correspond to a year during which ice-scars were recorded (Figure 7).

Eighteen (72%) of the 25 hydrographs associated with years of ice activity were characterized by these minimum values. In contrast, only one of the eight years with hydrographs that did not exceed any of the threshold values had an ice-push event. 1961 was characterized by a remarkably attenuated spring flood hydrograph. Half of the hydrographs related to years without ice-scouring were below the threshold values. Although there were few years without ice activity, this histogram (Figure 7) shows a downward trend in the number of hydrographs associated with the absence of ice-scars accompanying an increase in the number of threshold values exceeded.

Climatic conditions characterizing spring floods

Multiple regressions allowed for the identification of the main “climatic-period” variables that explained yearly variations in the total amount of water input during the months of May and June (Figure 8). It should be noted that the sum of water inputs in May and June combined was significantly correlated with both ice-scar frequency and maximum height ($r_s = 0.53$ and $r_s = 0.52$, respectively). According to the model, the sum of degree-days (DDH) of heat during winter months (October to April) had a strong

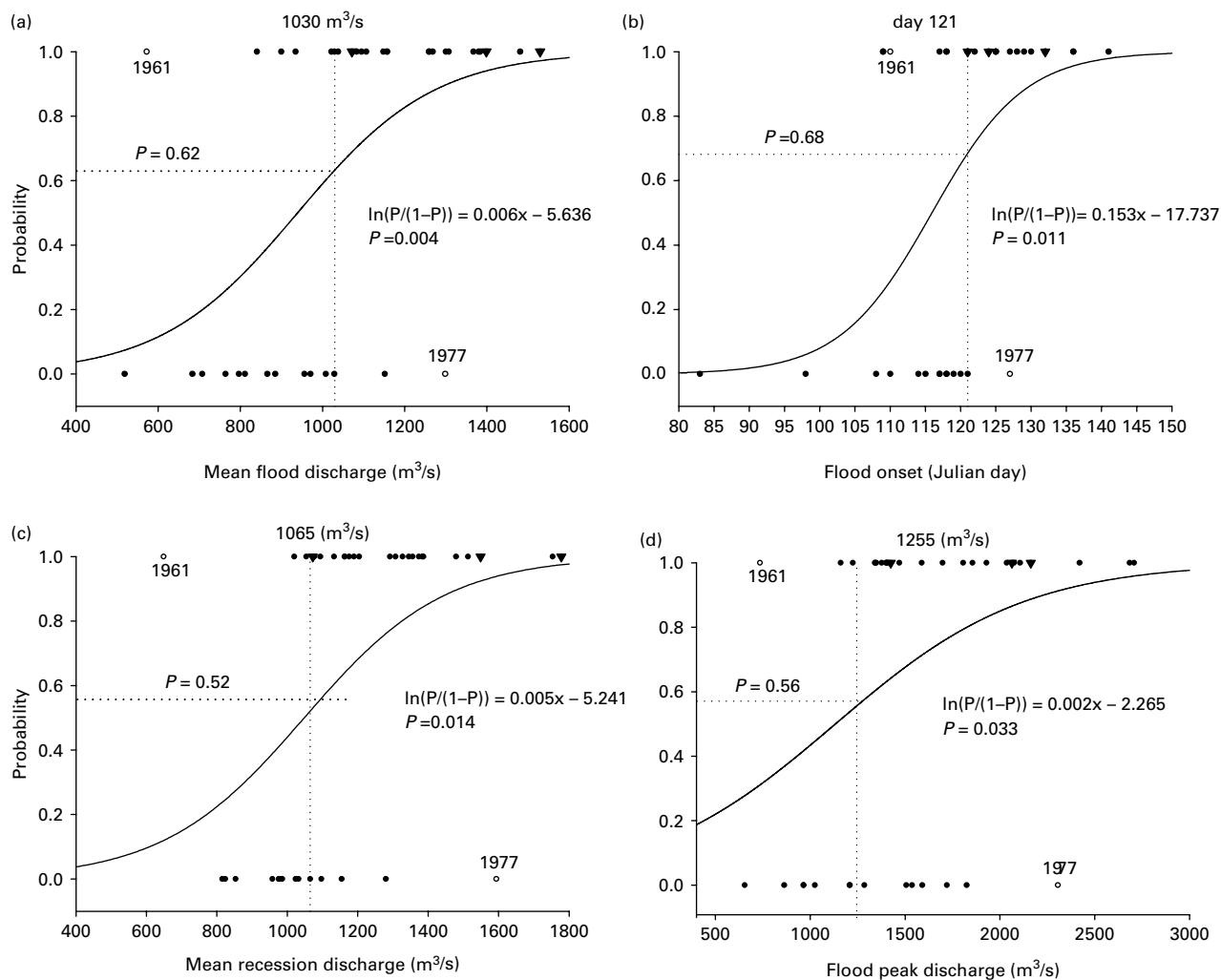


Figure 6 | Logistic predictive models of ice-push development according to the quantitative hydrograph variables (a: mean flood discharge, b: flood onset, c: mean recession discharge and d: flood peak discharge). The vertical axis represents the probability from 0 to 1 of ice-push occurrence. The dots correspond to the years with ($P = 1$) and without ($P = 0$) ice-scars, and inverted triangles represent major ice-pushes.

negative impact on water inputs at break-up time, while the sum of degree-days of frost (DDF) in early winter months (October to December) had a positive, but less significant, influence (Figure 8(a)). The model also indicated that spring precipitation was more significant than winter precipitation (January to March), although both were highly significant. These four climatic-period variables explained 72.3% of the variance in water input during the spring flood and were highly significant ($p < 0.001$).

Subsequent hydroclimatic analysis focused on June water inputs since Spearman's rank correlation suggested that ice activity was correlated with the sum of water inputs in June ($r_s = 0.57$; $p < 0.01$ and $r_s = 0.51$; $p < 0.01$

for ice-scar frequency and maximum height, respectively), while ice activity was not correlated with the sum of May water inputs. Five "climatic-period" variables were retained in the model, which was highly significant ($p < 0.0001$) and explained 72.9% of the variability in June water inputs (Figure 8(b)). Total precipitation during the winter months (January to March) and during the spring flood (May and June) were positively correlated with June water inputs, while April rainfall had a negative influence, although it was less significant. The sum of DDF in April had a positive effect on June water inputs. Finally, the model revealed that the sum of winter DDH (October to April) had a highly significant negative influence on June water inputs.

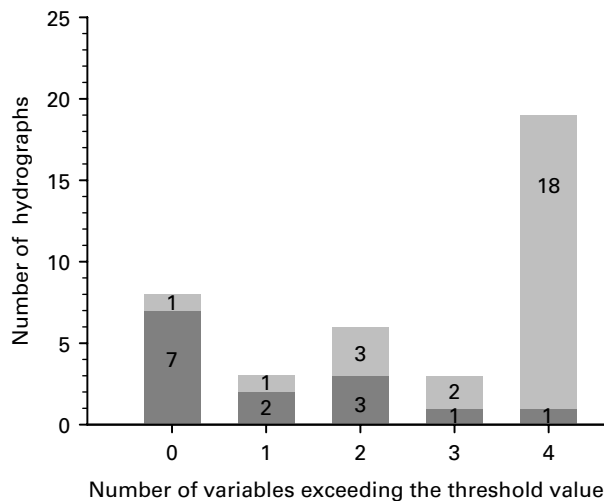


Figure 7 | Frequency of hydrographs (vertical axis) according to the number of the four significant hydrograph variables (flood onset, mean flood discharge, mean recession discharge and flood peak discharge) exceeding or not (horizontal axis) the threshold values identified by the logistic regression models. For example, eight hydrographs (left bar) were below the four identified hydrograph threshold values, including one leading to an ice-push event. Light grey bars: years with ice scars; dark grey bars: years without ice scars.

DISCUSSION

Interpretation of the ice-scar chronology

A recurrent issue in dendrochronological studies is the interpretability of the earliest part of a chronology mostly due to (1) lower tree availability (aged trees) that yields a record of the studied process (Shroder 1978) and (2) to the possible bias associated with hidden scars (Tardif & Bergeron 1997). In the present study, the entire chronology is considered as interpretable because the curve of the cumulative percentage of riparian tree establishment (or tree availability) (Figure 3) is a sigmoid, which characterizes a natural undisturbed tree stand. This indicated that the age structure of the riparian tree stands has not been altered by the ice activity and that severe ice-pushes did not lead to massive tree mortality that could erase older events in the riparian tree stand included in the chronology. Moreover, most ice-scars remain open during the entire lifetime because the radial growth is very slow at the Corvette Lake latitude (Bégin 2000c). Indeed, most of the 121 hidden scars discovered during laboratory analyses were present on the callous margins developed following the formation of the visible scars. In addition, the relative frequency of hidden scars was relatively constant within the chronology.

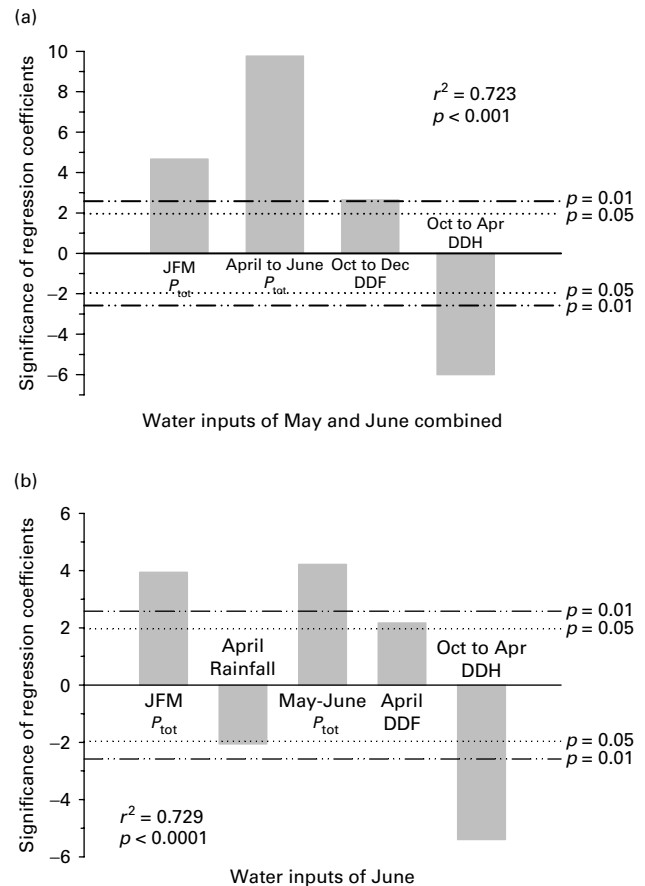


Figure 8 | Multiple regression models explaining the sum of water inputs in the LG3 reservoir (a) during May and June combined, and (b) during June. Note that in model (b), April precipitation was not included in May–June P_{tot} since (1) it had a negative influence on June water inputs and (2) since April snowfall did not have a significant influence on June water input, the variable used was April rainfall instead of April P_{tot} . JFM: January, February and March; DDF: degree-days of frost ($< 0^\circ\text{C}$); DDH: degree-days of heat ($> 0^\circ\text{C}$); P_{tot} : total precipitation. Negative values indicate negative correlations between regressors and dependant variables. P values are indicated by dotted lines ($p = 0.05$ and $p = 0.001$).

Consequently, hidden scars are not considered an element that could significantly influence the early part of the chronology.

The ice-scar chronology of Corvette Lake shares similarities with other published ice-scar records from large lakes in north-eastern Canada. Indeed, the chronology contains the same general rising trend during the 20th century observed at Bienville Lake (Lepage & Bégin 1996; Bégin 2000b), Clearwater Lake (Bégin & Payette 1988; Bégin 2000a) and Duparquet Lake (Tardif & Bergeron 1997). It showed a shift in the ice-scar frequency at the beginning of the 1930s, which has been highlighted by

Bégin (2000b) in both Bienville and Clearwater Lakes in the subarctic. In Duparquet Lake in the boreal zone, such a shift corresponded to 1870 and it was followed by an increase in the frequency of severe events around 1930. Bégin (2000b) hypothesized that, prior to 1930, low lake levels due to a lower snowfall regime prevented ice-pushes of similar severity to those seen between 1930 and 1980. Furthermore, some major ice-push events recorded in Corvette Lake also occurred in northern Québec, in particular the flood of 1979, an extreme flood recorded all across Canada in both lacustrine and fluvial environments (Payette 1980). In Clearwater Lake and Bienville Lake, 1959 was also characterized by many ice-scars as well as several traumatic, narrow and incomplete rings, indicating a high spring flood level (Lepage & Bégin 1996). The ice-push of 1947 was marked by abundant ice-scars in both Bienville (Bégin 2000b) and Duparquet lakes (Tardif & Bergeron 1997), while the ice-pushes of 1956 and 1957 were well marked in Duparquet Lake only.

Despite these similarities, the ice-scar chronologies at the finest temporal resolution yield many contrasts in the frequency, magnitude and synchronicity of ice-push events, which can be interpreted as regional and/or local differences in flood regimes due to spatial variability in precipitation (Bégin 2000b). In addition, the role of ice decay processes in the development of ice activity could exacerbate the contrasts between the chronologies because these processes can differ greatly between lakes according to their environmental context (latitude, location in the watershed, size and fetch, depth, shape, etc.). Bilello (1980) noted that some lakes experienced regular decay patterns from year to year, while others, mainly those with a large fetch, varied in ice regimes with time. Furthermore, Elo (2006) observed that ice break-up can be related to lake morphology, although this event mainly depends on air temperature.

Spring flood and ice-push relationships

The strong correlations between ice-push indicators and some hydrograph variables confirmed that drifting ice activity is directly linked to regional spring hydrology. In lacustrine environments, both ice-scar weighted frequency and scar height appeared to be better proxy indicators of

mean flood discharge than of maximum discharge, which was the hydrologic aspect of the flood considered “by default” in previous studies (Dionne 1979; Bégin & Payette 1988; Tardif & Bergeron 1997; Bégin 2000b). The fact that scar height was more strongly correlated to peak discharge than to scar frequency could indicate that maximum discharge has a strong impact on the rising of lake level, which probably reaches its maximum at the same time. Since peak discharge is a short-lived event, it has a lesser effect on scar frequency.

The time to peak and the slope of hydrograph rise were not correlated with ice activity indicators. This lack of correlation may be related to the ice decay processes that prevail in large lakes. In contrast to rivers, where mechanical break-ups are related to a rapid rise in runoff, amplified by high snowmelt rates and abundant rains (Smith & Pearce 2000; Beltaos 2003), in lakes there are no hydrodynamic forces accompanying a rapid rise that could cause ice-push development. In a large lake, ice cover decay depends mostly on incoming radiation, and the shear required to cause the ice cover to break up is provided only by the wind (Williams 1968; Ashton 1986; Elo 2006). However, it has been hypothesized that most ice-pushes occur while ice cover is still thick and strong enough to bear wind action without breaking up (Bégin 2000a). Ice-pushes occur during the intermediate phase of ice decay, before the ice cover reaches its weakest state during which the ice is candled and mottled, and can be physically broken up by the wind due to the loss of its structural integrity (Bulatov 1970; Ashton 1984; Bégin 2000a).

The relationship between the start of hydrograph rise and the ice-scar indicators is harder to explain. It could be postulated that ice conditions at the beginning of ice decay of an earlier flood are unfavorable to ice-push development (i.e. the ice cover is not deteriorated enough to be moved freely by the wind). An alternative explanation could be that early floods are usually less concentrated (or less intense) and such conditions could prevent the lake level from reaching the elevation required to cause ice-scouring, due to the drainage capacity of the lake outlet (Tardif & Bergeron 1997; Bégin 2000b).

The *t*-tests demonstrated that there was a clear hydrological distinction between floods that led to the development of ice-push and those that did not. However, the

hydrological differences that characterized severe ice-pushes were less obvious due to the lower profile of the flood of 1989. Many factors could explain why this flood led to a major ice-push event. Bégin (2000b, 2001) has shown evidence of regional differences in flood regimes at the subarctic–boreal interface. Accordingly, Corvette Lake possibly underwent a more important flood in 1989 than the rest of the LG3 reservoir watershed. This local hydrological signal would have been smoothed in the resulting regional hydrograph since Corvette Lake represents only 11.8% of the total area that supplies the LG3 reservoir (28,490 km²). However, it remains difficult to evaluate this hypothesis without local hydrological records. Regardless, spatial variability of flood regimes is postulated to be a factor that could partly explain some discordance between the regional hydrograph of the LG3 reservoir and the drifting ice activity of Corvette Lake (e.g. the floods of 1961 and 1977).

Another hypothesis that could explain the major ice-push recorded in Corvette Lake in spite of the relatively attenuated flood in 1989 is the possibility of an ice-jam in its outlet. The hydrograph of 1989 indicated that it was a very sudden flood. As mentioned previously, such a rapid rise could have triggered a mechanical break-up in the rivers surrounding Corvette Lake, leading to conditions that caused an ice-jam in its outlet (Sigafos 1964; Beltaos 2000; Smith & Pearce 2002). This would have considerably increased and maintained the lake level during flooding in spite of low or normal flood discharge. In addition, particularly strong and constant winds during flooding in 1989 could have amplified the impact of drifting ice on riparian trees, increasing ice-scar frequency only. The maximum scar height of 1989 was not greatly increased relative to other years with ice-scouring.

Integration of ice-scars as a discontinuous discrete parameter in a hydrological model

Logistic regressions were successfully applied to quantify the relationship between the significant hydrograph variables and drifting ice activity in Corvette Lake. Seventy-two percent of the hydrographs that led to an ice-push or ice-pushes or an ice-push event exceeded the four threshold values identified, indicating that the occurrence of

ice-scouring could be predicted with relative certainty. However, the prediction of years without ice scouring remains problematic, since only 50% of the hydrographs that did not lead to ice activity were below the four threshold values. Consequently, ice-scars could be integrated in a hydrological model as a discontinuous discrete parameter. This problem of discontinuity in the record provided by ice-scouring has already been discussed by Lepage & Bégin (1996), who concluded that the interpretation of this proxy indicator must be complementary to other dendrochronological indicators.

Climatic interpretation of spring flood hydrology

Previous studies conducted on ice floods in high-boreal and subarctic regions suggested that the rising trend of extreme stream flows and lake levels may result from an increase in snowfall during the early winter months (Bégin & Payette 1988; Payette & Delwaide 1991; Bégin 2000b, 2001). However, climatological analyses from the LG3 reservoir showed that the amount of input from the spring flood does not depend on snowfall during these early months, but partially depends on the interannual variation in snowfall during January–February–March. This agrees with the results found at Duparquet Lake (Tardif & Bergeron 1997), where spring precipitation (from April to June) was also closely related to the spring flood magnitude.

Degree-days of heat (DDH) and degree-days of frost (DDF) may influence soil drainage processes and subsequent river discharge. Hillel (1998) suggested that the permeability of soils is affected by freezing because ground ice impedes infiltration. According to Suzuki *et al.* (2006) spring flood discharge is mainly the result of snowmelt water infiltration and the maximum snow water equivalent (i.e. maximum snow cover). Colder temperatures favor ice formation in soils, which reduces water infiltration as well as drainage (Robock *et al.* 1998; Cherkauer & Lettenmaier 1999; Cherkauer *et al.* 2003). Consequently, severe and subsequent frost events during early winter can contribute to spring water inputs by stocking water at the soil surface. Furthermore, if the soil is partially or completely frozen during snowmelt, the infiltration capacity or the maximum infiltration rate is considerably reduced, which generates more surface runoff (Mitchell & Warrilow 1987; Cox *et al.* 1999).

As a result, the amount of water available during the spring flood increases. Conversely, warm temperatures in early winter slow the soil freezing rate, causing soils to remain permeable much longer, allowing infiltration and reducing the available amount of water for spring flood due to gravitational drainage (Cherkauer *et al.* 2003). Suzuki *et al.* (2006) observed that 22.9–61.5% of the maximum snow water equivalent can be absorbed in topsoil, which affects the generation of snowmelt discharge. Finally, low soil ice content allows for percolation of water made available by snow-thaw events in late winter. Indeed, measurements of mid-latitude soil moisture show that soil moisture fluctuates during winter as much as in other seasons (Vinnikov & Yeserkepova 1991; Vinnikov *et al.* 1996). Such conditions (e.g. warm temperatures in early and late winter) can contribute to decreases in the total discharge of the spring flood, which may help to explain the strong negative impact of the sum of DDH from October to April on spring flood water inputs, and especially on water availability for June runoff.

The stronger correlation between ice activity indicators and June water inputs suggested that climatic conditions surrounding ice activity differ slightly from those that simply lead to a high flood magnitude. These main differences, involving rainfall and the sum of DDF in April, indicated that climatic conditions during this month play a significant role in determining the timing of flood occurrence. Rainfall events combined with warm temperatures can provoke a sudden flood (Sigafos 1964; Payette 1980; Bégin & Payette 1988; Tardif & Bergeron 1997; Beltaos 2000, 2003). In the LG3 reservoir, abundant rainfall in April concentrates water inputs in May instead of June. Conversely, cold temperatures in April should delay the spring flood, increasing June water inputs.

CONCLUSION

In the absence of other proxy indicators, and given that no hydrological signal could be associated with ice-scouring intensity, the quantitative interpretation of our chronology (prior the period covered by the hydrological records) was limited to the threshold values identified to be associated with ice-push occurrence. From a hydrological perspective, the shift in the intensity of ice-push regimes at the turn of

the 1930s can be directly interpreted as an increase of spring flood water inputs in the watershed of the LG3 reservoir. The frequency of floods exceeding a mean flood discharge of 1,030 m³/s, a mean recession discharge of 1,065 m³/s, a peak discharge of 1,255 m³/s and that began after Julian day 121, increased following 1930.

The ice-scar chronology constructed from Corvette Lake suggests a shift in the ice-push regime at the turn of the 1930s. Our study supports the hypothesis that this shift could result from an increase in flood discharge. Hydrological analysis indicated that scar frequency and maximum scar height were reliable indicators of mean recession and mean flood discharge, peak discharge and the start of the hydrograph rise. Logistic regression assisted in quantifying the relationship between ice-push occurrence and these hydrograph variables. However, hydrological significance cannot be assigned to the absence of ice-scouring traces, as the lack of traces does not, in itself, necessarily imply the absence of a spring flood ice-push. Ice-scars can only be used as a discontinuous discrete parameter in a multivariate hydrologic forecast model. Replication of similar uses of ice-scar chronologies is needed to refine the classification of ice-push events in order to improve the quantitative prediction capabilities of this proxy indicator.

ACKNOWLEDGEMENTS

This study was supported financially by Hydro-Québec, the Ouranos Consortium, the National Sciences and Engineering Research Council of Canada (NSERC), the Department of Indian and Northern Affairs Canada, the Fonds Québécois de Recherche sur la Nature et les Technologies (FQRNT) and ArcticNet. We thank Jean-Sébastien Brulotte, Cédric Paitre, Véronique Tremblay and Antoine Nicault for assistance with field work, laboratory and data analyses. We also thank Dermot Antoniades and Christine Barnard for linguistic revisions. Comments from three anonymous reviewers were also appreciated on earlier versions of this manuscript.

REFERENCES

- Alestalo, J. 1971 Dendrochronological interpretation of geomorphic processes. *Fennia* 105, 1–141.

- Alestalo, J. & Häikiö, J. 1975 Ice features and ice-thrust shore forms at Luodonselkä, Gulf of Bothnia, in winter 1972/73. *Fennia* **144**, 1–24.
- Ashton, G. D. 1984 Deterioration of floating ice covers. In: *Proc. 3rd Int. Offshore Mechanics and Arctic Eng. Symp., New Orleans* Vol. 3, ASME International, New York, pp. 26–33.
- Ashton, G. D. 1986 *River and Lake Ice Engineering*. Water Resources Publications, Littleton, CO.
- Bégin, Y. 2000a Augmenting the potential for reconstruction of lake ice-floods using tree-ring records. In: *Proc. Int. Workshop on River Env. Considering Hydraulic and Hydrologic Phenomena in Snowy and Cold Regions* INRS-Eau, Québec, pp. 141–144.
- Bégin, Y. 2000b Ice-push disturbances in high-boreal and subarctic lakeshore ecosystems since AD 1830, northern Québec, Canada. *Holocene* **10**, 173–185.
- Bégin, Y. 2000c Reconstruction of subarctic lake levels over past centuries using tree rings. *J. Cold Reg. Eng.* **14**, 192–212.
- Bégin, Y. 2001 Tree-ring dating of extreme lake levels at the subarctic-boreal interface. *Quatern. Res.* **55**, 133–139.
- Bégin, Y. & Payette, S. 1988 Dendroecological evidence of lake-level changes during the last three centuries in subarctic Québec. *Quatern. Res.* **30**, 210–220.
- Beltaos, S. 2000 Advances in river ice hydrology. *Hydrol. Process.* **14**, 1613–1625.
- Beltaos, S. 2003 Threshold between mechanical and thermal break-up of river ice cover. *Cold Reg. Sci. Technol.* **37**, 1–13.
- Bilello, M. A. 1980 *Maximum Thickness and Subsequent Decay of Lake, River and Fast Sea Ice in Canada and Alaska*. CRREL Report. US Army Cold Reg. Res. Eng. Lab., Hanover, NH, pp. 80–86
- Bulatov, S. N. 1970 *Calculating the Strength of Thawing Ice Cover and the Beginning of Eind-activates Ice Drift* (in Russian). Engl. transl. Internal report 799. US Army Cold Reg. Res. Eng. Lab., Hanover, NH.
- Cherkauer, K. A. & Lettenmaier, D. P. 1999 Hydrologic effects of frozen soils in the Upper Mississippi River basin. *J. Geophys. Res.* **104**(D16), 19599–19610.
- Cherkauer, K. A., Bowling, L. C. & Lettenmaier, D. P. 2003 Variable infiltration capacity cold land process model updates. *Global Planet. Change* **38**, 151–159.
- Cox, P. M., Batts, R. A., Bunton, C. B., Essery, R. L. H., Rowntree, P. R. & Smith, J. 1999 The impact of new land surface physics on the GCM simulation of climate and climate sensitivity. *Climate Dyn.* **15**, 183–203.
- Dionne, J.-C. 1979 Ice action in the lacustrine environment. A review with particular reference to subarctic Quebec, Canada. *Earth-Sci. Rev.* **15**, 185–212.
- Efron, B. 1979 Bootstrap methods: another look at the jackknife. *Ann. Stat.* **7**, 1–26.
- Elo, A.-R. 2006 Long-term modelling of winter ice periods for morphologically different lakes. *Nordic Hydrol.* **37**, 107–119.
- Fritts, H. C., Blasing, T. J., Hayden, B. P. & Kutzbach, J. E. 1971 Multivariate techniques for specifying tree-growth and climate relationships and for reconstructing anomalies in paleoclimate. *J. Appl. Meteorol.* **10**(5), 845–864.
- Gregory, K. J. & Walling, D. E. 1973 *Drainage Basin Form and Process, A Geomorphological Approach*. Edward Arnold, London.
- Guiot, J. 1999 *3Pbase: Programs for Paleoecology and Paleoclimatology*. Institut Méditerranéen d'Ecologie et de Paléocécologie, CNRS, Marseille.
- Guiot, J., Berger, A. L., Munaut, A. V. & Till, C. I. 1982 Some new mathematical procedures in dendroclimatology, with examples from Switzerland and Morocco. *Tree-Ring Bull.* **42**, 33–48.
- Harrison, S. P. & Reid, O. E. 1967 A flood-frequency graph based on tree-scar data. *Proc. North Dakota Acad. Sci.* **21**, 23–33.
- Hillel, D. 1998 *Environmental Soil Physics*. Academic Press, New York.
- Karl, T. R., Groisman, P. S., Knight, R. W. & Heim, R. R. Jr. 1993 Recent variations of snow cover and snowfall in North America and their relation to precipitation and temperature variations. *J. Climate* **6**, 1327–1344.
- Lavoie, L. & Sirois, L. 1998 Vegetation changes caused by recent fires in the northern boreal forest of eastern Canada. *J. Veg. Sci.* **9**, 483–492.
- Lepage, H. & Bégin, Y. 1996 Tree-ring dating of extreme water level events at lake Bienville, Subarctic Québec, Canada. *Arctic Alpine Res.* **28**, 77–84.
- Mitchell, J. F. B. & Warrilow, D. A. 1987 Summer dryness in northern mid-latitudes due to increased CO₂. *Nature* **341**, 132–134.
- Parker, M. L. & Jozsa, L. A. 1973 Dendrochronological investigations along the Mackenzie, Liard and South Nahanni rivers, NWT. Part 1: Using tree damage to date landslides, ice jamming and flooding. In: *Hydrologic Aspects of Northern Pipeline Development*. Task Force on Northern Oil Development, Report 73-30, pp. 313–464.
- Payette, S. 1980 Les grandes crues glacielles de la rivière aux Feuilles (Nouveau-Québec): une analyse dendrochronologique. *Nat. Can.* **107**, 215–225.
- Payette, S. & Delwaide, A. 1991 Variations séculaires du niveau d'eau dans le bassin de la rivière Boniface (Québec nordique): une analyse dendroécologique. *Géogr. Phys. Quatern.* **45**, 59–67.
- Robock, A., Schlosser, C. A., Vinnikov, K. Y., Speranskaya, N. A. & Entin, J. K. 1998 Evaluation of AMIP soil moisture simulations. *Global Planet. Change* **19**, 181–208.
- Schweingruber, F. H. 1988 *Tree Rings. Basic and Applications of Dendrochronology*. Reidel, Dordrecht.
- Schweingruber, F. H. 1996 *Tree Rings and Environment Dendrochronology*. Paul Haupt Berne, Swiss Federal Institute for Forest, Snow and Landscape, Berne.
- Shroder, J. F. 1978 Dendrogeomorphological analysis of mass movement on Table Cliffs Plateau, Utah. *Quatern. Res.* **9**, 168–185.
- Shroder, J. F. 1980 Dendrogeomorphology: review and new techniques of tree-ring dating. *Prog. Phys. Geog.* **4**, 161–188.
- Sigafoos, R. S. 1964 *Botanical Evidence of Floods and Floodplain Deposition*. Prof. Paper 485A. US Geological Survey, Reston, VA.

- Smith, D. G. & Pearce, C. M. 2000 River ice and its role in limiting woodland development on a sandy braid-plain. *Wetlands* **20**, 347–367.
- Smith, D. G. & Pearce, C. M. 2002 Ice-jams caused fluvial gullies and scour holes on northern river flood plains. *Geomorphology* **42**, 85–95.
- Smith, D. G. & Reynolds, D. M. 1985 Tree scars to determine the frequency and stage of high magnitude river ice drives and jams, Red Deer, Alberta. *Can. Water Res. J.* **8**, 77–94.
- Suzuki, K., Kubota, J., Ohata, T. & Vuglinsky, V. 2006 Influence of snow ablation and frozen ground on spring runoff generation in the Mogot Experimental Watershed, southern mountainous taiga of eastern Siberia. *Nordic Hydrol.* **37**(1), 21–29.
- Tardif, J. & Bergeron, Y. 1997 Ice-flood history reconstructed with tree-rings from the southern boreal forest limit, western Québec. *Holocene* **7**, 291–300.
- Vinnikov, K. Y. & Yeserkepova, I. B. 1991 Soil moisture: empirical data and model results. *J. Climate* **4**, 66–79.
- Vinnikov, K. Y., Robock, A., Speranskaya, N. A. & Schlosser, C. A. 1996 Scales of temporal and spatial variability of midlatitude soil moisture. *J. Geophys. Res.* **101**, 7163–7174.
- Williams, G. P. 1968 Freeze-up and break-up of fresh-water lakes. In: *Proc. Conf. Ice Pressures Against Structures, Québec*. Technical Memorandum 92, National Research Council of Canada, Ottawa, pp. 203–215.

First received 12 December 2006; accepted in revised form 10 February 2008